Title
New twist in the optical schematic of surface slope measuring long trace profiler

ISBN
9781510612273

Authors
Nikitin, SM
Gevorkyan, GS
McKinney, WR
et al.

Publication Date
2017

DOI
10.1117/12.2274400

Peer reviewed

New twist in the optical schematic of surface slope measuring long trace profiler

Sergey M. Nikitin*[a], Gevork S. Gevorkyan[a], Wayne R. McKinney[b], Ian Lacey[a], Peter Z. Takacs[c], and Valeriy V. Yashchuk[a]

[a]Lawrence Berkeley National Laboratory, Advanced Light Source, One Cyclotron Road, Berkeley, CA 94720, USA; [b]Diablo Valley College, 321 Golf Club Rd, Pleasant Hill, CA 94523, USA; [c]Brookhaven National Laboratory, P.O. Box 5000, Upton, NY 11973-5000

ABSTRACT

The advents of fully coherent free electron lasers and diffraction limited synchrotron storage ring sources of x-rays are catalyzing the development of new, ultra-high accuracy metrology methods. To fully exploit the potential of these sources, metrology needs to be capable of determining the figure of an optical element with sub-nanometer height accuracy. Currently, the two most prevalent slope measuring instruments used for characterization of x-ray optics are the auto-collimator based nanometer optical measuring device (NOM) and the long trace profiler (LTP) using pencil beam interferometry (PBI). These devices have been consistently improved upon by the x-ray optics metrology community, but appear to be approaching their metrological limits. Here, we revise the traditional optical schematic of the LTP. We experimentally show that, for the level of accuracy desired for metrology with state-of-the-art x-ray optics, the Dove prism in the LTP reference channel appears to be one of the major sources of instrumental error. Therefore, we suggest returning back to the original PBI LTP schematics with no Dove prism in the reference channel. In this case, the optimal scanning strategies [Yashchuk, Rev. Sci. Instrum. 80, 115101 (2009)] used to suppress the instrumental drift error have to be used to suppress a possible drift error associated with laser beam pointing instability. We experimentally and by numerical simulation demonstrate the usefulness of the suggested approach for measurements with x-ray optics with both face up and face down orientations.

Keywords: x-ray optics, optical metrology, surface slope profilometry, LTP, pencil beam interferometry, Dove prism, error reduction, ZEMAX simulation.

1. INTRODUCTION

The advents of fully coherent free electron lasers and diffraction limited synchrotron storage ring (DLSR) sources of x-rays are catalyzing the development of x-ray optical elements and optical systems with extremely high performance, generally of diffraction limited quality, capable of delivering light to experiments without significant degradation of brightness and coherence. We need x-ray optics with residual (after subtraction of an ideal shape) surface slope and height errors of < 50-100 nrad (root-mean-square, rms) and < 1-2 nm (rms), respectively, with tight requirements to the allowed power spectral density and correlation lengths of errors. In addition, we have a strong need for nano-focusing optics significantly curved in the tangential (along the beam) direction and for 3-dimensional (3D) profiled mirrors with extremely high sagittal (across the beam) curvature; these are for optics with lengths up to one meter. Optimal usage of such x-ray optics in a beamline optical system requires high accuracy mutual positioning (~ 50 μm) and angular alignment (~ 50 μrad).

To fully exploit the potential of these x-ray sources and dedicated optics, new ultra-high accuracy ex situ metrology methods which are capable of determining the figure of an optical element with sub-nanometer height accuracy and sub-50-nrad slope accuracy, are needed (see, for example, Ref.[1] and references therein).The role of ex situ metrology is to assure the quality of the optical components mounted in a steerable support, installed in beamlines, and used as a part of the experimental systems. This entails measuring mirrors to ensure vendor compliance to specifications, verifying that the quality of the optical surfaces is not degraded when the optics are assembled and cooled, and thorough mutual alignment of optical components, tuning, and characterization of the opto-mechanical systems.

* smnikitin@lbl.gov; phone 1 510 286-4514; fax 1 510 486-7696

Usage of different instruments ex situ enables us to separately investigate and address different potential sources affecting beamline performance of an optic. These are surface quality (figure and finish errors), temporal and temperature dependence of surface shape, mechanical stability, gravity effect, alignments (twist, roll-off, yaw error), etc. All the perturbations at the beamline produce a cumulative effect to the performance of the optic that makes it difficult to optimize the optic's operational performance. The ex situ metrology allows us to fix a majority of problems before the installation of the optic at the beamline and to provide feedback on design and guidelines on usage of optics (e.g., ambient temperature stability and accuracy of alignments).

Currently, the two most prevalent slope measuring instruments used to characterize x-ray optics are the auto-collimator based NOM (nanometer optical measuring device[2,3]) like system[2-8] and the long trace profiler (LTP)[9-19] using pencil beam interferometry (PBI).[20] These devices have been consistently improved upon by the x-ray optics metrology community, but appear to be approaching their metrological limits (see, for example, Refs.[21-24] and references therein). The current performance of the slope metrology is close to the requirements for the state-of-the-art x-ray optics for only measurements with close to plane (R > 100 m) and relatively small optics. The accuracy achieved in slope measurements with significantly curved (100 > R > 10 m) and sagittally shaped optics is worse by a factor of about 2-3 than the typical specification for optics for FELs and DLSR sources limited by instrumental systematic errors. A detailed analysis of the systematic errors in surface slope measurements can be found, for example, in Refs.,[22,25-27] where a comprehensive literature review is also presented (see also Sec. 2, below).

Here, we report on our recent experience using the Advanced Light Source (ALS) LTP-II[19] for measurement with different beamline optics that directed us to revise the traditional optical schematic of the PBI-based LTP[14] by removing the Dove prism in the LTP reference channel. The main advantage apparent is the elimination of the systematic error related to the fabrication imperfection of the Dove prism. We show that the function of the Dove prism in the LTP schematic to provide control for the light beam pointing instability can be successfully reassigned to the proper arrangement of the LTP measurement run by using optimal scanning strategy method[28] developed for suppression of the errors due to random noise and temporal drift.

In the next section, Sec.2, we review the development of the PBI based LTP optical schematic and analyze the factors limiting the LTP performance. In Sec. 3, we show that at the level of accuracy desired for metrology with state-of-the-art x-ray optics, the Dove prism in the LTP reference channel appears to be one of the sources of uncertainty of the LTP metrology. Therefore, we suggest returning back to the original PBI LTP schematics with no Dove prism in the reference channel. In sec. 4, we compare the performance of the reference arm of the ALS LTP-II with and without Dove prism. Section 5 is the conclusion providing a discussion of our current and future directions for development.

2. PENCIL BEAM INTERFEROMETRY BASED SURFACE SLOPE PROFILOMETRY

With the example of the optical sensor of the ALS upgraded LTP-II,[19] Fig. 1 depicts a typical schematic of a long trace profiler based on pencil beam interferometry.

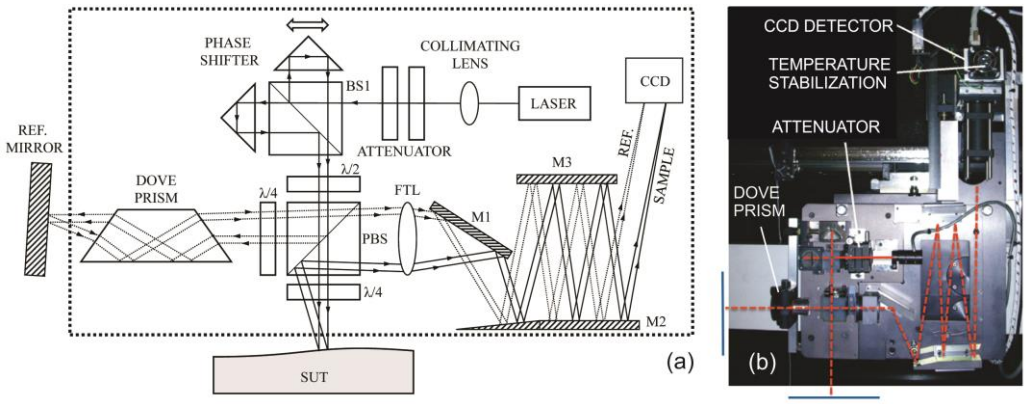

Figure 1. Optical sensor of the ALS upgraded LTP-II.[19] The used abbreviations are explained in the text.

In the ALS LTP-II, the sensor elements shown in Fig. 1a within the dotted box are placed on an air-bearing carriage, moving in the course of measurement along the surface under test, SUT. In Fig. 1a, BS1 is a beam splitter used to split

the laser beam to two interfering 'pencil' beams. With the help of the movable and stationary Porro prisms constituting the phase shifter, we can adjust the phase difference and spatial separation of the two beams. The beam splitter BS2 sends the two-component beams to the SUT (the sample beam) and to the stationary reference mirror (the reference beam). The reflected sample and reference beams are focused with the Fourier transform lens, FTL, to the focal plane where a position sensitive CCD detector records the intensity distribution resulting from the interference of two components of each beam. Usually, the phase difference is selected to be equal π, determining the distractive character of the interference with intensity distribution with a minimum in the center. The FTL is designed to linearly transform the beam tilt angle to its lateral position in the focal plane. Therefore, the position of the central minimum is used as a measure of the surface tilt/slope of the mirror that is a half of the angular deflection of the corresponding reflected beam. The fold mirrors, M1, M2, and M3, allow a relatively compact design at the FTL focal length of 1.25 m. The reference arm records the spurious slope variation appeared due to the carriage pitch wobbling, as well as pointing instability of the laser beam. The role of the Dove prism in the reference channel is to combine the errors due to the pitch wobbling and pointing instability with the same relative sign as they contribute to the slope variation measured in the sample arm (see also Sec. 3).

Below in this section, we briefly review the major developments of the LTP optical design and discuss the factors limiting the current performance of the pencil beam interferometry based surface slope profilers.

2.1 Development of optical design of pencil beam interferometry based long trace profilers: brief historical review

Pencil beam interferometry as a technique for profiling surfaces was initially suggested by K. Von Bieren in 1982.[29-31] The application of the PBI in long trace profilers for precision characterization of x-ray mirror surface slope topography was first suggested by P. Takacs, et. al.[32] in 1987. The first optical design of the LTP[32-34] that did not include a reference arm, suffered of the pitch variation of the instrumental translation system. The magnitude of the pitch error can reach more that 10-20 μrad (see, for example, Refs.[14,35]).

An additional straightness reference arm with a stationary reference mirror (without a Dove prism) was introduced in 1991 by S. Irik et. al.[12] It was mistakenly stated that simple subtraction of the signal in the reference arm from the sample signal allows removing both, the carriage pitch wobbling and light beam pointing instability errors. The mistake was pointed out by S. Irick in Ref.,[13] where he suggested to separately measure the carriage pitch error and laser beam pointing instability with an additional reference arm.

A thorough analysis of the "out-of-phase" combination of carriage wobbling and laser beam pointing instability in the LTP reference arm compared the sample arm was provides by P. Takacs and C. Bresloff [36] in 1996 (see also Ref.[14]). They suggested an elegant solution of the problem by adding into the reference beam a Dove prism, attached to the LTP optical head as shown in Fig. 1a. The addition of the reference arm with the Dove prism basically completed the development of the LTP optical design, leading to significant improvement of the precision (repeatability) of the LTP measurements bring it to the system noise level of ~ 1 μrad (rms) (see, for example, discussion in Ref.[14]). Paradoxically, further improvement of LTP performance to the level of modern requirements of <0.1 μrad must overcome a number of disadvantages inherent, in particular, to the optical reference channel. Among the disadvantages are the limited quality of the additional optics and air convection noise due to the long optical path (see, for example, discussion in Refs.[19,22]).

2.2 Development of experimental methods and techniques for suppression/elimination of the LTP random noise, drift and systematic errors

In spite of the fact that by the early 21st century the precision of the LTP measurements achieved sub-micro radian level, the accuracy still remained at a few micro radians, as determined by the systematic errors due to the imperfections of the instrument's optical elements, lack of proper calibration methods, low frequency random noise, and set-up drift error. The global problem with accuracy of the LTP measurements was clearly illuminated, for example, in the results of a round robin survey of some LTPs within the United States performed by S. Irick in 1999 with a set of concave and convex spherical reference mirrors with radius of curvature of about 40 m.[37] The overall difference of the residual (after subtraction of the best fit spherical shape) slope variation measured at the different facilities reached more than 10 μrad. The variation of the measured values of the radius of curvature appeared to be about 1%, corresponding to the radius of the effective (spurious) curvature of some LTP systems participated in the survey of about 4 km!

Therefore, given the LTP schematic basically unchanged, the efforts of the synchrotron metrology community was then directed to development of experimental methods and techniques for suppression/elimination of the LTP random noise,

drift and systematic errors, where us the basic optical schematic of the LTP system was generally not changed. The next round robin survey, undertaken in 2006 by F. Siewert, et al.,[38] has demonstrated noticeably smaller variation of the measurements carried out at different facilities.

2.2.1 LTP random error

The main source of random error of an LTP is air convection along the optical path of the reference and sample arms, as caused by temperature gradients and air flow.[38] Due to air convection (turbulence) the refractive index of the air along the optical paths changes, leading to pointing instability of the light beams. Because the optical paths of the sample and the reference beams are different, the corresponding errors do not correlate and cannot be accounted by the optical reference channel. The air-convection error can be suppressed by shielding of the LTP optical paths. However, application of an adequate shielding to the reference arm is difficult (if not impossible) because of its continuous change during a measurement scan.

The intensity of the air convection, as well as the overall stability of an optical profiler system, are strongly correlated with environmental conditions in the lab. For this reason, the new ALS X-ray Optics laboratory[39] (XROL) is constructed to keep the cleanroom laboratory at temperature of approximately 20 ºC with the long term (over a few days) stability of about ±30 mK. Additional temperature insulation of the LTP-II set-up with surrounding hutch and curtain systems drops the temperature variation over the measuring set-up to the level of a few mK. Never the less, the resulting random error of the slope reading in the reference channel is still rather large of about 0.3 μrad/Hz$^{1/2}$. This can be due to the unavoidable air flow from the carriage air-bearing system.

The air convection noise has a low frequency characteristic with typical frequencies of 0.1-1 Hz.[38] Therefore, for efficient suppression of the noise by averaging the repeated measurements, the interval between the averaged measurements has to be much larger than 10 sec. Below, we show that suppression of the instrumental drift systematic errors can be achieved by averaging multiple measurements performed under controlled changes of the parameters of the experimental set-up and scanning (direction of scanning, orientation, and alignment of the SUT, etc.). In this case, the low frequency random noise is also effectively averaged out.

2.2.2 Drift errors

Drift error appears as a very slow temporal variation of the measured quantity with a characteristic time comparable to the duration of the measurements. The main sources of drift error in LTP measurements are slow variations of the environmental conditions (temperature and, in some degree, humidity in the lab), and inherent temporal instabilities of the measurement setup (e.g., mechanical instability of the mirror mounting and alignment).

In the LTP-II optical designed shown in Fig. 1a, temperature instability around the two Porro prisms (e.g., due to the heat load from the CCD camera) can cause a drift of the phase difference between the two interfering beams and, therefore, a long term drift of the measured value of the surface slope of up to several micro radians (see, for example, Ref.[19]). Much more stable π-phase shifters designed as a stepped phase plate have been discussed in Refs.[40,41] However, a shifter of this type does not allow adjustment of the beam separation that found to be useful for optimization of the LTP operation.[42] (Note that we do not discuss here slope profilers with a single Gaussian beam[15,43] that do not belong to the class of the PBI based LTPs.)

The experimental method for effective suppression of spurious effects in slope measurements caused by slow instrumental drifts was suggested and first demonstrated in Ref.[28] According to the method, each measurement is an average of surface slope traces recorded in an optimally arranged set of sequential scans with the profiler in the forward (F) and backward (B) directions. For example, the scanning strategy F-B-B-F-B-F-F-B for a measurement run of 8 sequential scans is optimal for suppression of the contribution to the error of polynomial drifts up to the third order.[28] Additionally, the averaging efficiently suppresses the low frequency random noise due to air turbulence. A single run of 8 optimally arranged scans is usually enough to solve the problems of the drift error and random noise.

The pointing instability error, related to a change of temperature of the LTP diode laser, also has a character of a slow drift error (see, for example, Ref.[14]). A significant improvement can be obtained by replacing the diode laser with a fiber coupled temperature stabilized diode or He-Ne laser.[15,35] The tests described in Ref.[38] show that the low frequency (≤1 Hz) variations of pointing of a beam from a fiber coupled laser are less than 0.1 μrad (rms). As discussed in Sec. 2.1, the addition of the Dove prism to the reference arm allows accounting for the pointing instability error. Moreover, because of the typical drift character of the pointing error, it is effectively suppressed in the measurements performed according to the optimal scanning strategies, discussed above (see also Sec. 4).

2.2.3 LTP systematic errors

As pointed out above, the major limited factors of the modern LTP systems are systematic errors, which are systematically reproduced in identical scans and, therefore, cannot be suppressed by averaging over repeated measurements performed with an unchanged experimental arrangement. Due to the inherent repeatability of the systematic error, people can hope to calibrate the error in the dedicated test measurements. However, due to the strong dependence of the systematic errors on a particular measurement arrangement including the specifics of the SUT surface shape and size (see, for example, Refs.[19,44] and references therein), the thorough calibration of slope profilers (useful for all potential experimental arrangements and SUT's shapes) with different types of angular generators[44-46,] is extremely difficult, if not impossible. An additional problem, due to the LTP angular dynamic range, typically runs almost over six orders of magnitude from a few hundredths of microradians to ten milliradians.

There were suggested a number of calibration methods that are specific to the particular measurements.[47-49] The drawback of the dependence of the systematic errors on the specific measurement arrangement can be advantageous if people use the correlation method for suppression of systematic errors of slope profilers, as suggested in Ref.[25] The reliability and efficiency of the calibration of a slope profiler can be significantly improved by using the SUT as a reference mirror (self-reference) when calibrating the profiler, avoiding the need for a universal multi-dimensional calibration, accounting for all possible shapes of SUTs. A prototype of a tilting stage capable for accommodation large x-ray mirror substrates is in use at the HZB/BESSY optics lab.[23] Unfortunately, the stage is designed with the tilt pivot point that cannot be placed on the mirror surface, as it would be in the case of an optimal tilting stage dedicated to the self-reference measurements.

In the terms of a specific spatial frequency range, the systematic errors of an LTP can be divided into two groups, as distinguished by the spatial frequency range at which they perturb. One group relates to the uncertainty of the instrumental calibration, corresponding to relatively lower spatial frequencies. Such an error appeared, for example, due to aberration of the Fourier transform lens or out-of-focus position of the CCD detector, can be relatively easy calibrated with a slope generator.

The other group of systematic errors relates to the quality of the instrument's optical elements contributing to the error at relatively higher spatial frequencies. These include the systematic errors due to optical homogeneity of materials used in the beam splitters, Fourier transform lens, the Dove prism, the quality of the reflecting surfaces of the mirrors and mirror prisms,[9] and the components of the CCD detector system.[50] In a slope trace measured with the LTP, these systematic errors appear as local (relatively high spatial frequency) perturbations with amplitudes up to 1 μrad and larger. Besides simply improving quality of the optical elements, there are experimental methods to decrease the contribution due to the high spatial frequency systematic errors. For example, one can perform multiple measurements with the same SUT, but with different arrangements (pitch and roll tilt, lateral position, and orientations) with respect to the instrument's optics and detector.[22,25] For an optimal set of measurements, the systematic perturbation would appear at different locations along the slope traces and could be reduced by averaging over the measurements. Practically speaking, the high frequency systematic errors in measurements with strongly curved x-ray optics can be suppressed to a level below 0.25 μrad (rms).[39,48]

A radical solution for elimination of the systematic errors due to the homogeneity of materials and shape quality of the LTP optical components is to develop the LTP schematic with reduced amount of the optical elements. For example, in our LTP depicted in Fig. 1, we use an FTL with focus length of 1250 mm that dictated the usage of the fold mirrors. Using an FTL with shorter focus length (about 500 mm), we can design the LTP optical head without the fold mirrors.

Below in Secs. 3 and 4, we demonstrate that due to the application of the optimal scanning strategy method,[28] the drift error due to the laser pointing instability is suppressed to the level when we can remove the Dove prism without losing the measurement accuracy. In some sense, this is a 'new' twist on the old optical schematic of the LTP, when instead of adding new elements for improving the LTP accuracy, we remove the previously essential elements to get higher performance of the instrument.

3. DOVE PRISM IN THE ALS LTP-II REFERENCE CHANNEL

The major property of a Dove prism is to invert an image passing through the prism without lateral transposition that would appear in the case of inversion in one reflection from a mirror). The inversion includes image flipping used in the

LTP in order to change the sign of the carriage pitch wobbling error measured in the reference arm, as suggested in Refs.[14,38] (see also Fig. 1a).

However, the Dove prism in the LTP reference channel correctly combines the errors only in measurements with an SUT oriented face-up. It was almost immediately recognized[51] that in the measurements with face-down SUT, when two pentaprisms added to the sample arm, the wobbling and pointing instability errors in the reference arm are originally (without the Dove prism) combined with the same relative sign as they contribute to the slope variation measured in the sample arm.[51] For the measurements with side-facing SUT, the Dove prism should be rotated around the direction of the reference light beam by 45 degrees.[51] The latter result relates to the known rotation property that the image transmitted by a Dove prism rotated along their longitudinal axis rotates at twice the rate of the prism. Note that in the LTP case (Fig. 1a), the polarization rotation property of the Dove prism[52-54] does not affect the intensity in the reference arm because of the Dove prism deals with a circular polarized light.

The addition of the Dove prism to the LTP optical schematic significantly improves the precision (repeatability) of the LTP measurements, bringing it to the level limited by the air convection noise. But as we show below in this section on the example of the Dove prism used in the reference arm of the ALS LTP-II, the fabrication imperfections of the real Dove prism level out the positive effect leading to new systematic errors that critically depends on mutual alignment of the Dove prism and the reference mirror.

3.1 Dependence of the ALS LTP-II reference measurements on (mis)alignment of the reference mirror

Working with our LTP-II, we empirically found that the slope variation measured in the reference arm significantly depends on alignment of the optical components in the reference arm. To minimize the dependence, we use an alignment procedure comprising of three steps.

First, with Dove prism removed we align the reference laser beam to be parallel to the axis of translation of the LTP carriage. To perform the alignment, we place a CCD camera in the position of the reference mirror. The camera monitors the variation of the reference light beam position while the carriage is translated over the entire scanning range of the LTP-II of about 1 m. By the precise tilting of the diode laser, we find the laser angular alignment corresponding to the minimum of peak-to-value (PV) variation of the beam position on the CCD camera.

Next, with the Dove prism in place and using the same CCD camera to monitor the reference beam position as above, we align the Dove prism with the goal to keep the reference laser beam to be parallel to the axis of the carriage translation.

Finally, with the camera removed we align the reference mirror mounted on a precise kinematic stage. In this case, an iris diaphragm is mounted on the carriage right after the Dove prism. The diaphragm is centered to the center of the beam passed the Dove prism. In the course of aligning the reference mirror, we intend to center the reflected beam to the diaphragm orifice. In spite of the fact that we select the maximum distance between the reference mirror and the carriage, this is the less precise part of the alignment procedure because of the subjective character of the alignment by a naked eye. We estimate the accuracy and repeatability of the reference mirror alignment to be about 0.1-0.2 mrad.

Fig. 2 shows the slope traces measured in the ALS LTP-II reference arm at two different alignments of the reference mirror undistinguished with the current alignment procedure.

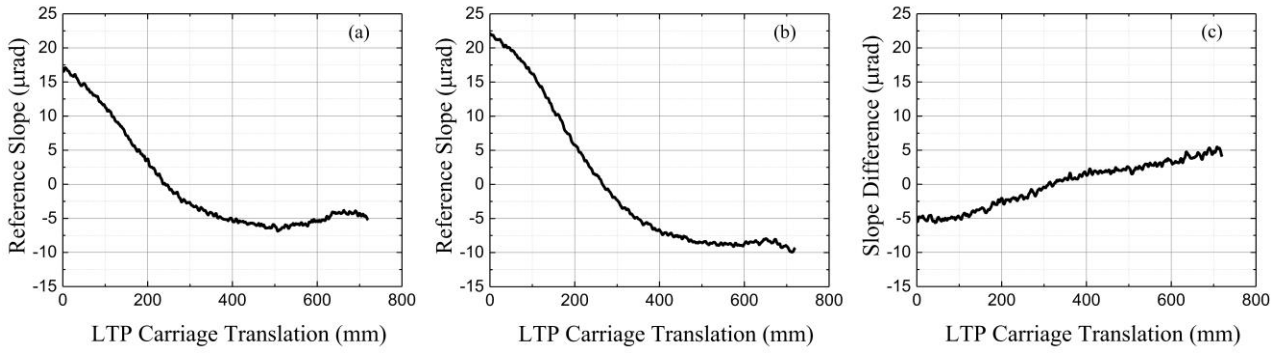

Figure 2. Measurements with the reference arm of the ALS upgraded LTP-II[19] when (a) the reference mirror and the Dove prism are nominally aligned using the procedure described in the text, (b) the same but the alignment of the reference mirror is slightly changed being still in the range of the alignment accuracy; and (c) the difference of the traces (a) and (b).

Each slope trace in Fig. 2 is the result of averaging of 4 sequential scans arranged according to the scanning strategy F-B-B-F, optimal for suppression of the polynomial drift errors up to the second order.[28] In particular, a linear drift error of the measurements is significantly suppressed. Nevertheless, the difference of the measurements with peak-to-value variation of about 10 μrad has a strong linear trend that can be characterized with an effective radius of curvature of ~65 km.

The contribution of the observed uncertainty of the measurements in the LTP-II reference arm to the uncertainty of the SUT shape metrology depends on the surface radius of curvature. For example, in the measurement with cylindrical mirrors with radius of curvature of 650 m and 6.5 km, the corresponding uncertainty of the measured radius is about 1% and 10%, respectively. Note that the ultimate stability of the current ALS LTP-II is characterized with the effective radius of curvature larger than at least 300 km (see also Sec. 4).

The observations, like the one depicted in Fig. 2, stimulated us to investigate the dependence of the LTP reference arm performance on the quality of the Dove prism and mutual alignment of the Dove prism and reference mirror.

3.2 Interferometric measurements with the Dove prism from the ALS LTP-II

Figure 3 shows the experimental arrangement of the measurements of the optical quality of the Dove prism from the ALS LTP-II with a ZYGO Verifire™ 6-in Fizeau interferometer available at the ALS XROL. In the measurements, the Dove prism was placed in the front of the interferometer and the transmitted light was reflected back to the prism with a high quality plane reference flat mirror. In order to increase the resolution, we used the zoom of about ×3. The curved interference fringes from the Dove Prism, seen in Fig. 3b, clearly indicate the effective cylindrical shape of the prism in its working direction. We empirically found that the best fringe pattern from the prism appears at prism tilt of about 45 degrees. This is probably due to the specific of the adjustable stage used to align the Dove prism. It also can be due to the polarization direction of the interferometer's light.

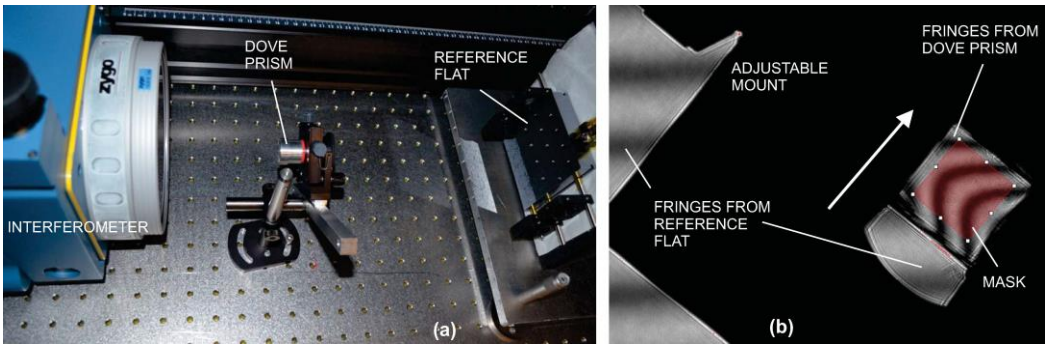

Figure 3. (a) Experimental arrangement of measurements of optical quality of the LTP-II Dove prism with ZYGO DynaFiz™ interferometer and (b) the observed interference fringe pattern. The curved fringes from the Dove Prism clearly indicate the effective cylindrical shape of the prism. The arrow shows the prism working direction. Note that fringes from the reference flat are also seen in an opening right below the prism.

Figure 4 depicts the result of measurements of the optical quality of our Dove prism with the ZYGO Verifire™ interferometer.

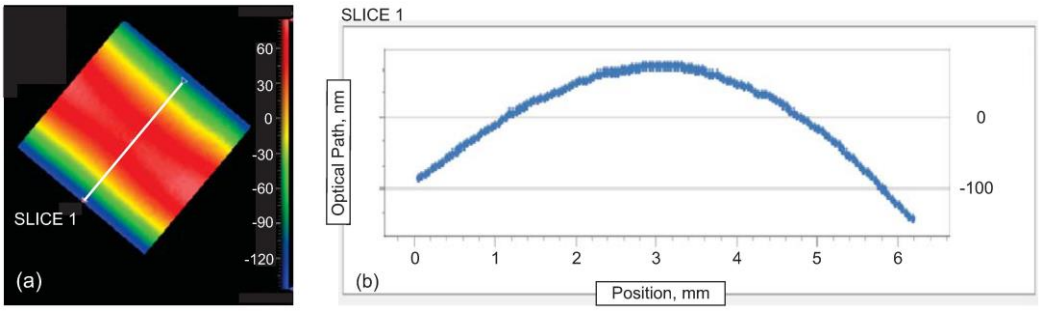

Figure 4. The effective optical shape of ASL LTP-II Dove prism as measured with the XROL ZYGO Verifire™ Fizeau interferometer: optical path variation (a) inside the mask in Fig. 3b and (b) along Slice 1 in the prism working direction.

The major observation from the measurement in Fig. 4 is the relatively large curvature of the wavefront of the light passed through the prism twice. In the working direction, the effective curvature of the wavefront perturbation is characterized with the radius of 26.5 m, concave. The observed curvature can be attributed to a deviation of the prism input and output surfaces from the desired plane shape that leads to the corresponding increase of the optical path. The Dove prism shape imperfection constitutes an equivalent cylindrical concave-flat lens in the reference arm. The radius of the concave surface of the leans if made of an optical glass with refractive index n=1.5 is 26.5 m. Below, we show that such a lens when added to the reference arm can leads to a significant error in monitoring of the LTP carriage wobbling.

3.3 ZEMAX simulations of the systematic error due to the limited optical quality of Dove prism

In order to understand the magnitude of the systematic error in the reference channel possible due to the limited optical quality of Dove prism, we performed ray trace simulations with ZEMAX™ optical design software.

Figure 5 presents a simplified schematic of the LTP reference arm used in the simulation. A thin plate splitter, BS1, deflects the laser beam to the reference arm with an ideal Dove prism and a reference mirror, M1. A concave/plane lens, L, is added to account for the observed surface curvature of the LTP-II Dove prism. The beam reflected from the reference mirror passed back through the lens, the Dove prism, and beam splitter is detected with a slope sensor consisting of a Fourier transform lens, FTL, and CCD detector, placed to the FTL focal plane at the distance of 1250 mm, corresponding to our LTP. For converting the position of the detected beam to the measured angle, we use the calibration coefficient of 0.4 μrad/μm.

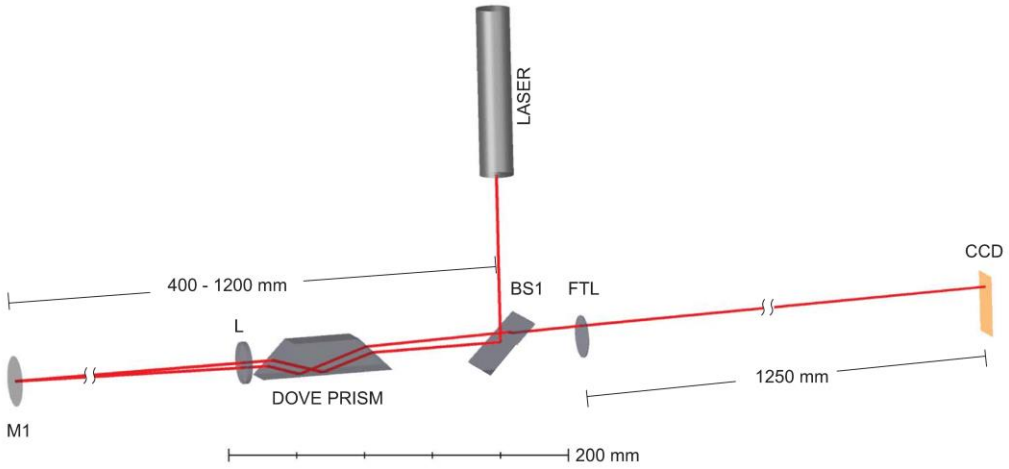

Figure 5. Simplified schematic of the LTP reference arm used in the simulation. The notations are discussed in the text.

In order to simulate the effect of carriage wobbling in the ray-trace calculation with ZEMAX software, we suppose that the wobbling has parabolic shape with effective radius of curvature of 30.8 km that corresponds to a linear variation of the carriage pitch angle from -13 μrad to +13 μrad when the carriage is translated by 800 mm. This range of the pitch angular variation roughly correspond to the range of the carriage wobbling measured with the ALS LTP-II reference arm as shown in Fig. 2. The wobbling can be thought of as a result of the limited quality of the gantry ceramic beam and its shape change due to the gravity. Note that the calculations in ZEMAX are easier if the carriage wobbling effect is transferred to the corresponding simultaneous tilt and translation of the reference mirror (Fig. 5).

3.3.1 Performance of the LTP reference arm in the case of an ideally aligned reference mirror

Figures 6 and 7 reproduce the result of ZEMAX calculation of the wobbling angle trace recorded with the CCD detector in the arrangement in Fig. 5 in the case of ideal alignment of the reference mirror. The ideal alignment corresponds to the normal orientation of the mirror with respect to the input light beam at the wobbling angle equal to zero. In the ZEMAX calculation this situation is simulated as scanning of the reference mirror pitch tilt angle by $\mp$ 13 μrad with zero offset.

The plot (a) in Fig. 6 shows the wobbling angle recorded without Dove prism in the reference arm. The corresponding measurement error equal to the difference between the recorded trace and the applied linear variation of the wobbling angle simulated as a linear variation of the pitch tilt of the reference mirror is depicted in plot (a) in Fig. 7. The observed small deviation of the error trace from a zero-error trace characterized with the variation of about 8 nrad (PV) appears

due to the dependence of the aberration of the Fourier transform lens on the distance from the FTL to the reference mirror. The FTL is designed for the optimal object distance of 500 mm specified for placing an SUT in the sample arm, whereas in our calculations the distance is varying from 400 mm to 1200 mm.

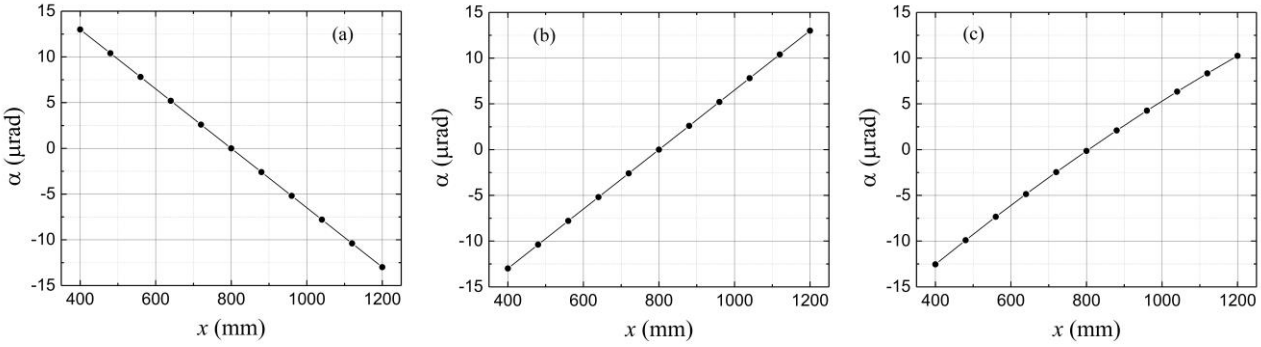

Figure 6. Result of ZEMAX calculation of the wobbling angle trace recorded with the CCD detector (in the arrangement in Fig. 5) in the case of ideal alignment of the reference mirror: (a) without Dove prism in the reference arm, (b) with an ideal Dove prism, and (c) with an ideal Dove prism and an additional cylindrical lens mimicking the Dove prism imperfections as described in the text above. The dots depict the calculated values; whereas, the solid lines connecting the dots are drawn to guide the eye.

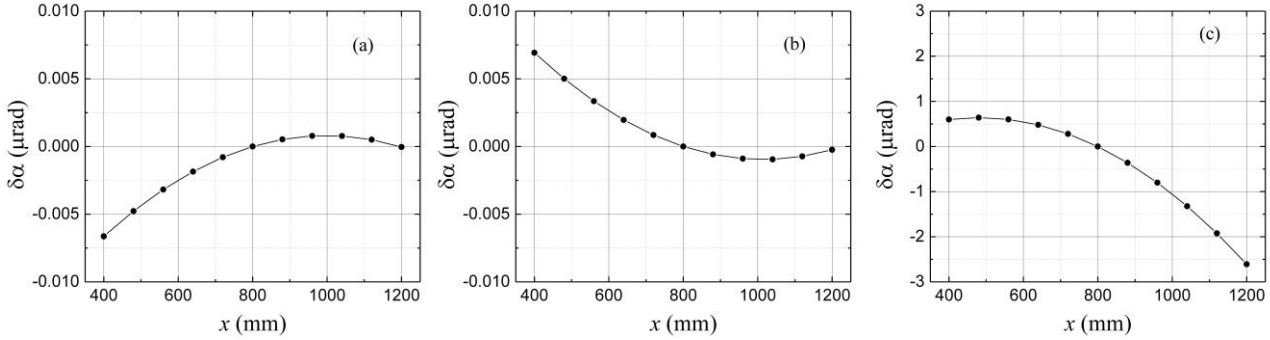

Figure 7. The traces of errors in the recorded wobbling angle calculated as a difference of the traces in Fig. 6 and the applied linear variation of the wobbling angle in the case of ideal alignment of the reference mirror: (a) without Dove prism in the reference arm, (b) with an ideal Dove prism, and (c) with an ideal Dove prism and an additional cylindrical lens imitating the Dove prism imperfections.

The addition of an ideal Dove prism to the reference arm expectantly flips the calculated wobbling angle trace (Fig. 6b) and does not affect the magnitude of the corresponding aberration error (Fig. 7b) compared to the case (a) without Dove prism.

In the case of an non-ideal Dove prism, imitated with the additional concave/plane lens with radius of curvature of 26.5 m (Figs. 6c and 7c), the error in the recorded wobbling trace is significantly larger, with variation of more than 3 μrad (PV). The radius of the corresponding spurious curvature, calculated from the best linear fit to the error trace in Fig. 7c, is about 249 km that produces a significant error in the figure measurements with plane and slightly curved x-ray optics (see the relevant discussion in Sec. 3.1).

3.3.2 Effect of reference mirror misalignment to performance of the LTP reference arm

A dramatic dependence of the error of the reference arm measurements on the misalignment of the reference mirror is illustrated in Figs. 8 and 9. Here, we present the results of the same set of ZEMAX calculations as in Figs. 6 and 7, but with the reference mirror pitch tilt offset Δ = -100 μrad. Without and with an ideal Dove prism (Figs. 8a, 9a and Figs. 8b, 9b, respectively), this misalignment results in increase of the error by a factor of approximately 7, reaching ~55 nrad (PV). In the case of the non-ideal Dove prism (Figs. 8c and 9c), the error becomes ~ 12 μrad (PV). The radius of the corresponding spurious curvature is now about 43 km that is comparable with the radius of curvature of 30.8 km corresponding to the carriage wobbling used in this simulations.

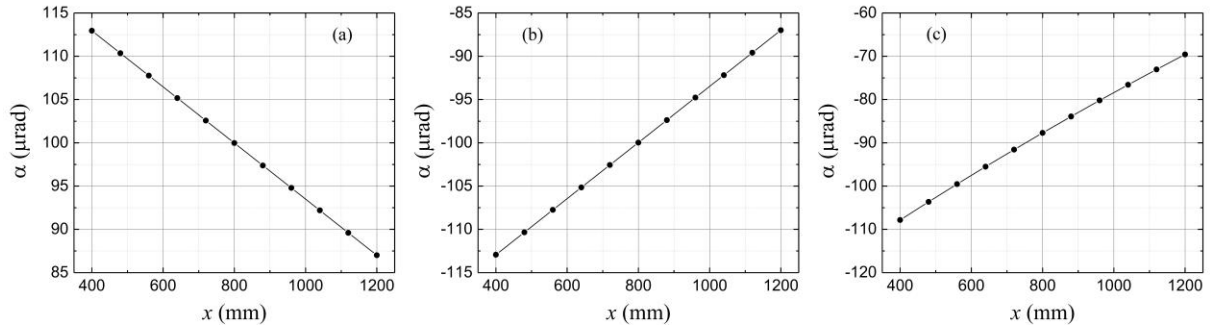

Figure 8. Result of ZEMAX calculation of the wobbling angle trace recorded with the CCD detector (in the arrangement in Fig. 5) in the case of misalignment of the reference mirror by Δ =-100 μrad: (a) without Dove prism in the reference arm, (b) with an ideal Dove prism, and (c) with an ideal Dove prism and an additional cylindrical lens mimicking the Dove prism imperfections as described in the text above.

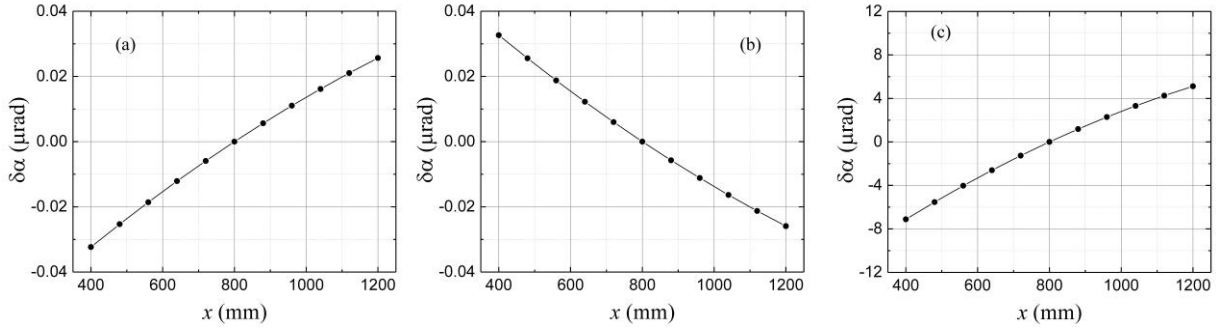

Figure 9. The traces of errors in the recorded wobbling angle calculated as a difference of the traces in Fig. 6 and the applied linear variation of the wobbling angle in the case of misalignment of the reference mirror by Δ =-100 μrad: (a) without Dove prism in the reference arm, (b) with an ideal Dove prism, and (c) with an ideal Dove prism and an additional cylindrical lens imitating the Dove prism imperfections.

3.3.3 Scaling of the spurious effect with the magnitude of the reference mirror misalignment

In order to understand the scaling of the spurious effect associated with misalignment of the reference mirror in the LTP equipped with an non-ideal Dove prism with the magnitude of the misalignment, we repeated the simulations depicted in Figs. 8 and 9 but with different misalignments: Δ = -200 μrad (Figs. 10 and 11), Δ = 100 μrad (Figs. 12 and 13), and Δ = 200 μrad (Figs. 14 and 15).

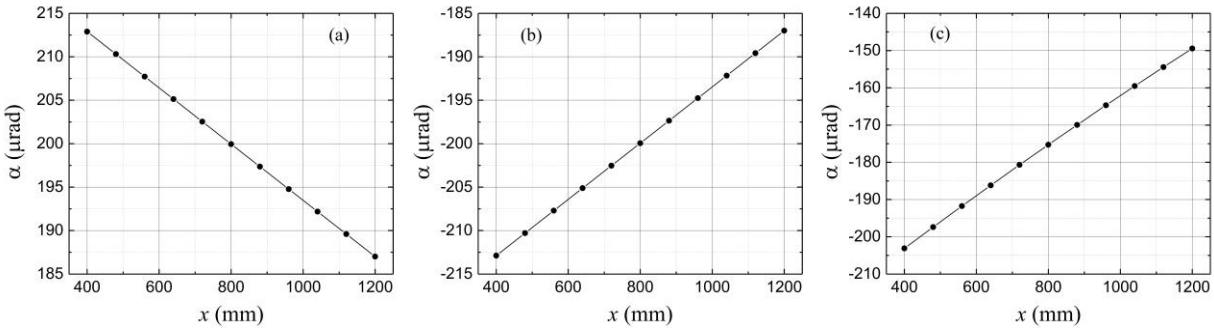

Figure 10. Result of ZEMAX calculation of the wobbling angle trace recorded with the CCD detector (in the arrangement in Fig. 5) in the case of misalignment of the reference mirror by Δ = -200 μrad: (a) without Dove prism in the reference arm, (b) with an ideal Dove prism, and (c) with an ideal Dove prism and an additional cylindrical lens mimicking the Dove prism imperfections as described in the text above.

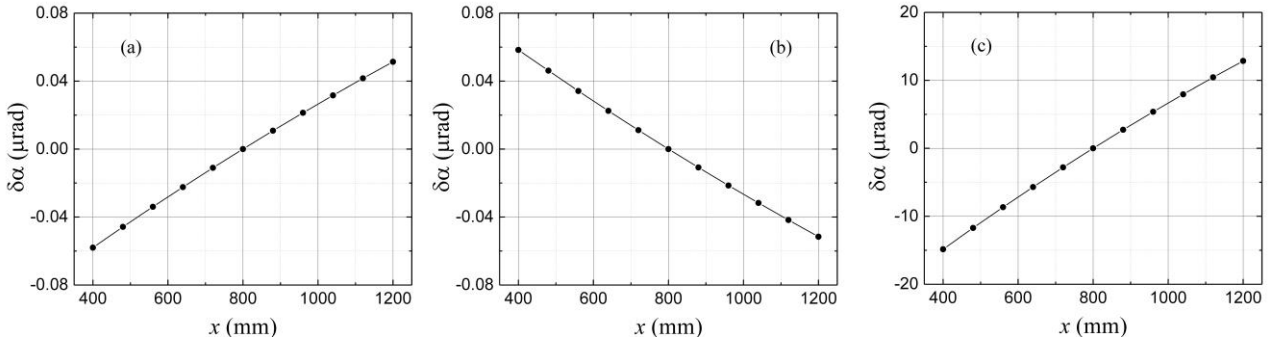

Figure 11. The traces of errors in the recorded wobbling angle calculated as a difference of the traces in Fig. 6 and the applied linear variation of the wobbling angle in the case of misalignment of the reference mirror by -200 μrad: (a) without Dove prism in the reference arm, (b) with an ideal Dove prism, and (c) with an ideal Dove prism and an additional cylindrical lens imitating the Dove prism imperfections.

Increase of the misalignment from Δ = -100 μrad to Δ = -200 μrad, lead to more than a factor of 2 growth of the PV error in the wobbling measurement with the non-ideal Dove prism, from 18 μrad to 35 μrad (compare Figs. 9c and 11c). For the LTP without Dove prism and with an ideal one, the error is still rather small, ~100 nrad (PV), having the similar growth by a factor of ~2.

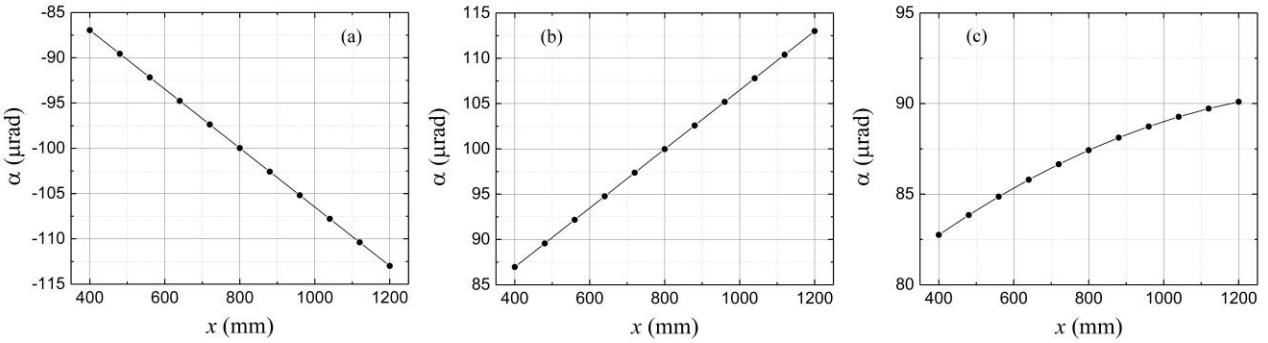

Figure 12. Result of ZEMAX calculation of the wobbling angle trace recorded with the CCD detector (in the arrangement in Fig. 5) in the case of misalignment of the reference mirror by Δ = 100 μrad: (a) without Dove prism in the reference arm, (b) with an ideal Dove prism, and (c) with an ideal Dove prism and an additional cylindrical lens mimicking the Dove prism imperfections as described in the text above.

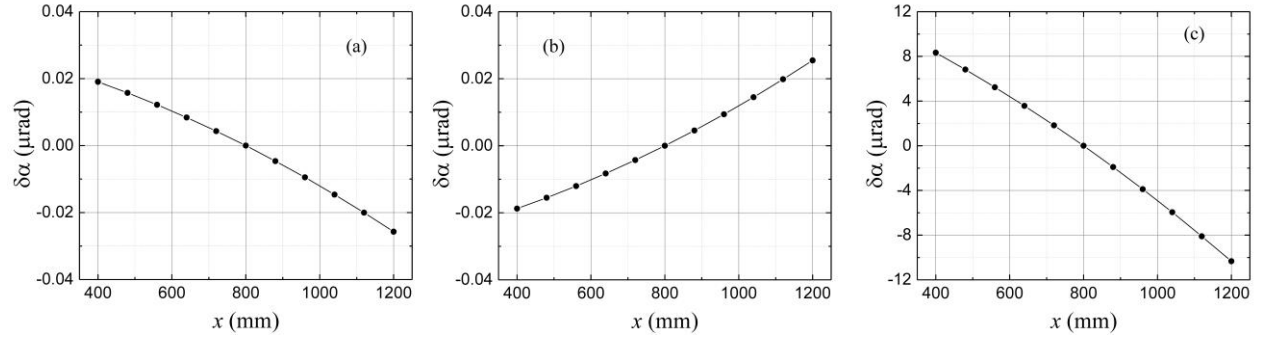

Figure 13. The traces of errors in the recorded wobbling angle calculated as a difference of the traces in Fig. 6 and the applied linear variation of the wobbling angle in the case of misalignment of the reference mirror by Δ = 100 μrad: (a) without Dove prism in the reference arm, (b) with an ideal Dove prism, and (c) with an ideal Dove prism and an additional cylindrical lens imitating the Dove prism imperfections.

Comparison of the results of the calculations with the misalignment of Δ = -100 μrad (Figs. 8 and 9) and Δ = 100 μrad (Figs. 12 and 13), shows a flip of the error sign and brings out a significant asymmetry of the error magnitudes. While the former observation is trivial, the latter one is less obvious. As discussed above, the misalignment of reference mirror appears as an offset of the linear pitch angle variation simulating the wobbling effect. Depending on the relative sign of the wobbling angle and the offset, the absolute value of the beam deflection can be larger at the larger or smaller distances between the reference mirror and the non-ideal Dove prism. Because the aberration effect increases with enlargement of the distance, the error becomes larger when the sign of the offset and wobbling angles is the same at larger distances. Therefore, there is an inherent asymmetry in the LTP measurement arrangement treated here with ZEMAX.

There is also a remarkable result related to the dependence of the sign of the error trace on the sign of the offset. In the arrangement of our ZEMAX calculations, at Δ=150 μrad, the error due to the imperfections of the Dove prism nearly compensates the angular variation due to the linear wobbling. This can be seen by comparing the result of the calculations at Δ = 100 μrad and Δ = 200 μrad depicted in Figs. 12, 13 and Figs. 14, 15, respectively. While the resulted reference traces have approximately the same PV variation of about 8 μrad (Figs. 12c and 14c), the tilt of the traces has opposite sign. Accordingly, the effective curvature measured in the reference arm with these two misalignments of the reference mirror has opposite sign.

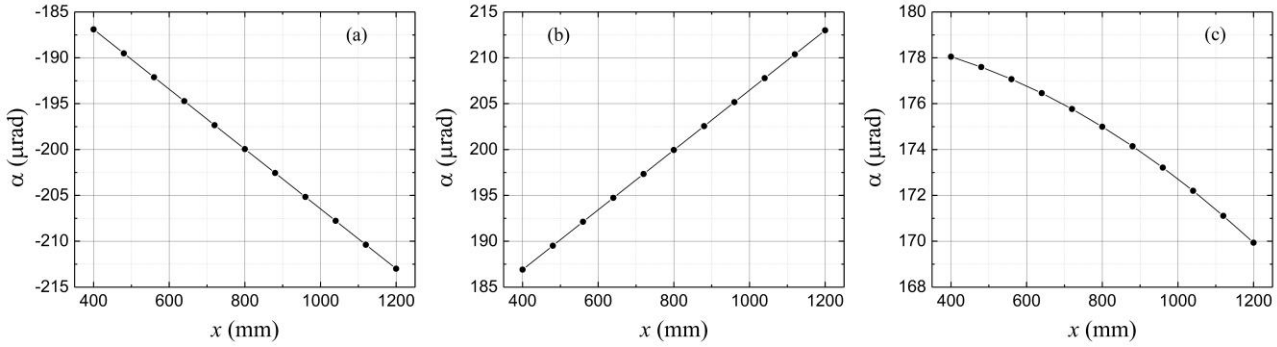

Figure 14. Result of ZEMAX calculation of the wobbling angle trace recorded with the CCD detector (in the arrangement in Fig. 5) in the case of misalignment of the reference mirror by Δ = 200 μrad: (a) without Dove prism in the reference arm, (b) with an ideal Dove prism, and (c) with an ideal Dove prism and an additional cylindrical lens mimicking the Dove prism imperfections as described in the text above.

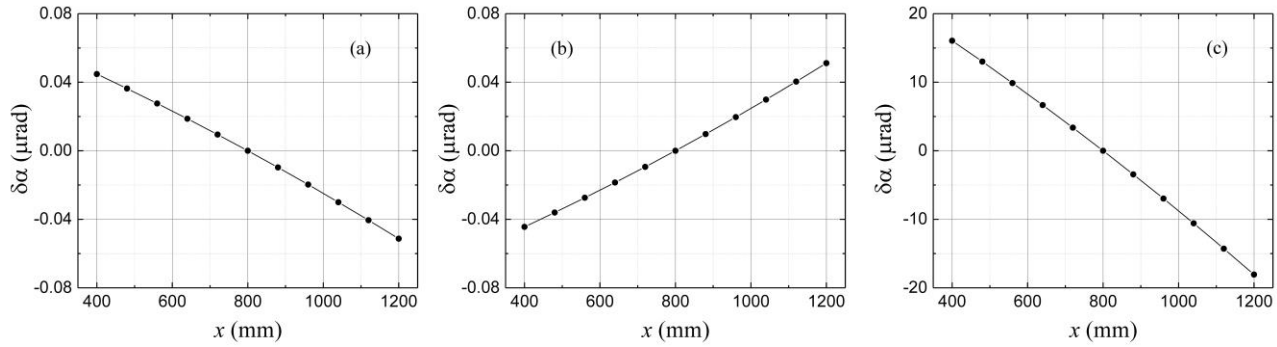

Figure 15. The traces of errors in the recorded wobbling angle calculated as a difference of the traces in Fig. 6 and the applied linear variation of the wobbling angle in the case of misalignment of the reference mirror by Δ=200 μrad: (a) without Dove prism in the reference arm, (b) with an ideal Dove prism, and (c) with an ideal Dove prism and an additional cylindrical lens imitating the Dove prism imperfections.

Figure 16 summarizes the discussed strong dependence of the effective reference curvature (obtained from the best linear fit of the reference arm slope traces calculated with non-ideal Dove prism in place) on the value of the reference mirror misalignment. According to our calculations, a relatively small misalignment (with the range of ±200 μrad) can lead to the effective curvature from zero to the curvature twice larger than that of due to the carriage pitch wobbling alone. These would impose one with a mistaken conclusion about the quality of the carriage translation stage ranging from almost ideal to unacceptably poor.

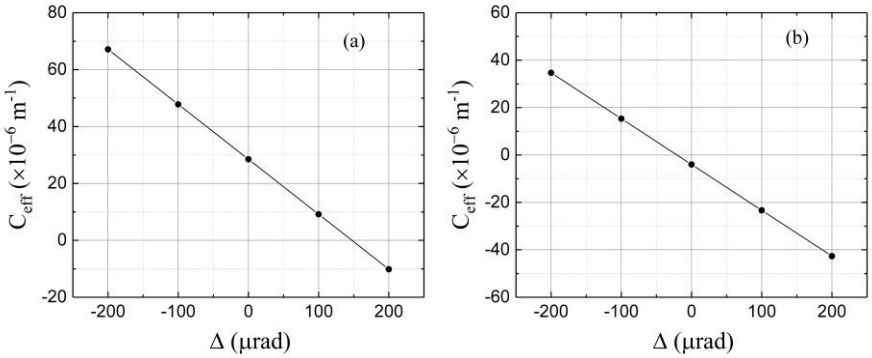

Figure 16. (a) Dependence of the effective curvature measured in the reference arm on the reference mirror misalignment. This should be compared with the curvature of 32.5×10^{-6} m^{-1} corresponding to the linear wobbling used in the ZEMAX calculations. (b) The spurious curvature obtained from the best linear fit of the error traces calculated for the case of the LTP equipped with the non-ideal Dove prism. The error nearly compensates the wobbling at the mirror misalignment Δ = 150 μrad.

4. PERFORMANCE OF THE ALS LTP-II REFERENCE ARM WITHOUT DOVE PRISM

ZEMAX ray-trace simulations discussed in Sec. 3 brought us to understanding that the uncertainty of alignment of the reference mirror significantly compromises the confidence of monitoring of the carriage wobbling in the ALS LTP-II equipped with a Dove prism with the known limited optical quality.

From other side, the investigations on suppression of other instrumental drift error previously performed suggest that the function of the Dove prism in the LTP schematic to provide control for the laser beam pointing instability can be successfully reassigned to the proper arrangement of the LTP measurement run by using optimal scanning strategy method[28] developed for suppression of the errors due to random noise and temporal drift.

At these circumstances we decided to make new twist in the LTP saga and return back to the original PBI LTP schematics with no Dove prism in the reference channel to reduce the systematic error caused by the imperfection of this optical element. The question is the stability and repeatability of reference arm measurements with the LTP without Dove prism. The answer can be found via comparison of experimental data in Figs. 17 and 18, where two pairs of identical consecutive measurements in the reference arm of the ALS LTP-II with (Fig. 17) and without Dove prism (Fig. 18). Each measurement is the average of 8 optimally arranged scans. The time delay between the measurements was at least one day.

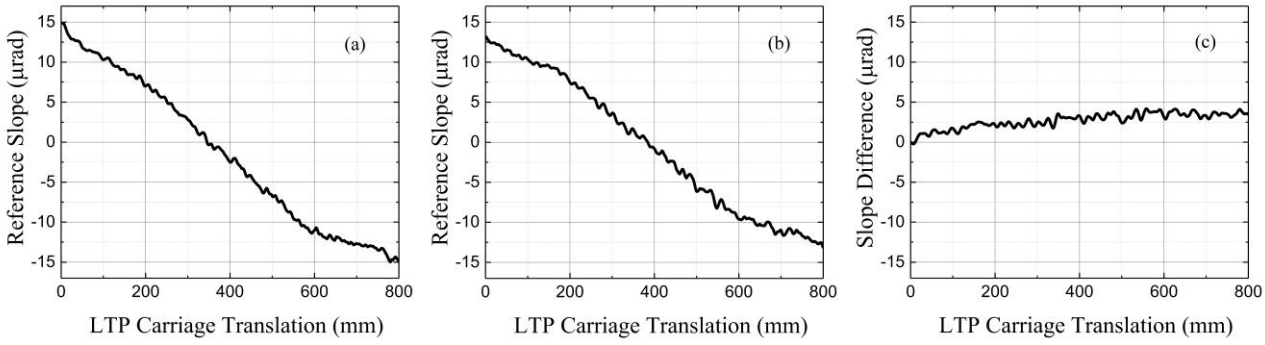

Figure 17. Reference arm repeatability test with ALS LTP-II equipped with the Dove prism characterized in Sec. 3: (a) and (b) two identical runs performed with more than 1 day delay; (c) the difference of the traces (a) and (b). The PV variation of the difference trace is about 4 μrad; the equivalent radius of curvature is 282 km.

In the case of the ALS LTP-II with the Dove prism, the difference between the two reference slope traces with a length of 800 mm (Fig. 17c) has the PV variation of about 4 μrad. The best linear fit of the difference suggests for the equivalent radius of curvature of 282 km. Note higher special frequency instability that is probably also associates with the optical quality.

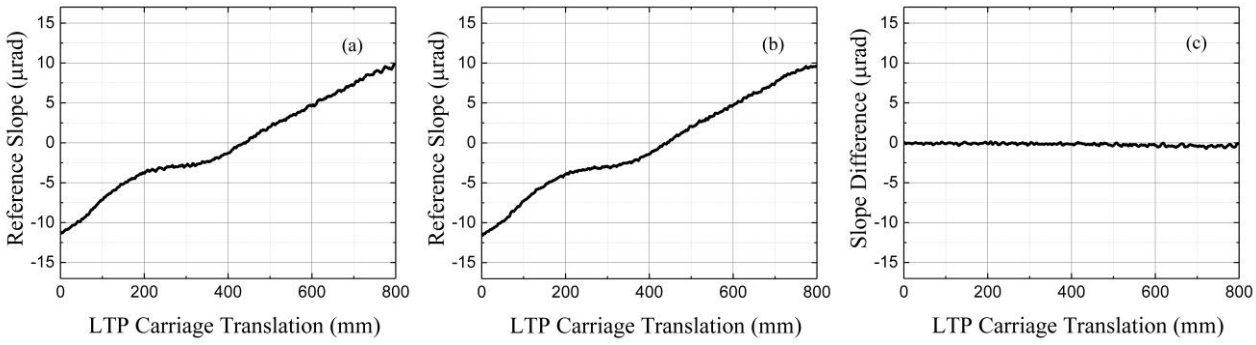

Figure 18. Reference arm repeatability test with ALS LTP-II without Dove prism: (a) and (b) two identical runs performed with more than 3 days of delay; (c) the difference of the traces (a) and (b). The PV variation of the difference trace is about 1 μrad; the equivalent radius of curvature is 2056 km.

The repeatability test carried out with the ALS LTP-II with removed Dove prism (Fig. 18) shows only ~1 μrad PV variation over the same length of the carriage translation of 800 mm. The best linear fit of the difference gives the equivalent radius of curvature of more than 2000 km. Therefore, the remove of Dove prism together with using suitable measurement strategy allows for required elimination of the systematic error associated with the prism without compromising the precision (repeatability) of the ALS LTP-II measurements in the reference arm.

5. CONCLUSIONS

A detailed study of the ALS LTP-II functioning via experimental observation and ZEMAX simulation, discussed in the present paper, has shown that one the main sources of systematical error is Dove prism in the reference arm. Numerical ray-tracing simulations performed with ZEMAX software have brought to the light a strong dependence of the error on misalignment of the LTP reference mirror. In these simulations, the measured cylindrical optical path distortion of the prism was mimicked with an equivalent concave/plane lens added to the reference arm.

At these circumstances we have made a new twist in the ALS LTP-II saga and returned back to the original PBI LTP schematics with no Dove prism in the reference channel. We have demonstrated that the combination of using optimal scanning strategy methods and removing Dove prism allows eliminating the systematic error associated with the prism without compromising the precision (repeatability) of the ALS LTP-II measurements in the reference arm.

The results of present work can also be thought of as a ‘smoking gun’ evidence for the possible problem with addition of a focusing lens in the sample arm with a goal to increase the spatial resolution of LTP measurements.[56] Similar to the effect of the week lens in the LTP reference arm imitating, in our case, imperfections of the LTP Dove prism, a focusing lens in the sample arm can course a significant measurement error strongly dependable on the shape of the SUT and its distance to the Fourier transform lens.

In the present work, we did not analyze one more possible source contributing to the error of wobbling measurement in the LTP reference arm equipped with non-ideal Dove Prism. These include the pitch misalignment of the Dove prism itself. ZEMAX simulations of this effect are in progress and will be reported elsewhere. Our plan for the next step is to build a comprehensive model of the LTP including interference effects with the goal of reanalysis and optimization of the pencil beam interferometry based surface slope profiler.

ACKNOWLEDGEMENTS

The Advanced Light Source is supported by the Director, Office of Science, Office of Basic Energy Sciences, Material Science Division, of the U.S. Department of Energy under Contract No. DE-AC02-05CH11231 at Lawrence Berkeley National Laboratory. Research at Brookhaven National Laboratory is sponsored by the U.S. Department of Energy under Contract No. DE-AC02-98CH10886.

REFERENCES

[1] Idir, M. and Yashchuk, V. V., Co-Chairs, "Optical and X-ray metrology," in [X-ray Optics for BES Light Source Facilities], Report of the Basic Energy Sciences Workshop on X-ray Optics for BES Light Source Facilities, D. Mills and H. Padmore, Co-Chairs, pp. 44-55, U.S. Department of Energy, Office of Science, Potomac, MD (March 27-29, 2013); http://science.energy.gov/~/media/bes/pdf/reports/files/BES_XRay_Optics_rpt.pdf.

[2] Siewert, F., Noll, T., Schlegel, T., Zeschke, T., and Lammert, H., "The Nanometer Optical Component Measuring machine: a new Sub-nm Topography Measuring Device for X-ray Optics at BESSY," AIP Conference Proceedings 705, American Institute of Physics, Mellville, NY (2004), pp. 847-850.

[3] Siewert, F., Lammert, H., Zeschke, T., "The Nanometer Optical Component Measuring Machine;" in: [Modern Developments in X-Ray and Neutron Optics], Edited by A. Erko, M. Idir, T. Krist, and A. G. Michette, Springer, New York (2008).

[4] Alcock, S. G., Sawhney, K. J. S., Scott, S., Pedersen, U., Walton, R., Siewert, F., Zeschke, T., Senf, F., Noll T., and Lammert, H., "The Diamond-NOM: A non-contact profiler capable of characterizing optical figure error with sub-nanometre repeatability," Nucl. Inst. and Methods A 616(2-3), 224-228 (2010).

[5] Nicolas, J., Martínez, J. C., "Characterization of the error budget of Alba-NOM," Nucl. Instr. and Meth. A 710, 24-30 (2013).

[6] Yashchuk, V. V., Barber, S., Domning, E. E., Kirschman, J. L., Morrison, G. Y., Smith, B. V., Siewert, F., Zeschke, T., Geckeler, R., Just, A., "Sub-microradian surface slope metrology with the ALS Developmental Long Trace Profiler," Nucl. Instrum. and Methods A 616(2-3), 212-223 (2010).

[7] Qian, J., Sullivan, J., Erdmann, M., and Assoufid, L., "Performance of the APS optical slope measuring system," Nucl. Instr. and Meth. A 710, 48-51 (2013); https://doi.org/10.1016/j.nima.2012.10.102.

[8] Qian, S., Geckeler, R., Just, A., Idir, M., and Wu, H., "Approaching sub-50 nanoradian measurements by reducing the saw-tooth deviation of the autocollimator in the Nano-Optic-Measuring Machine," Nucl. Instr. and Meth. A 785, 206-212 (2015); doi: 10.1016/j.nima.2015.02.065.

[9] Church, E. L., Takacs, P. Z., "Use of an optical profiling instrument for the measurement of the figure and finish of optical quality surfaces," Wear 109, 241-57 (1986).

[10] Takacs, P. Z., Qian, S., Colbert, J., "Design of a long trace surface profiler," Proc. SPIE 749, 59-64 (1987).

[11] Takacs, P. Z., Feng, S. K., Church, E. L., Qian, Shinan, Liu, W-M., "Long trace profile measurements on cylindrical aspheres," Proc. SPIE 966, 354-64 (1989).

[12] Irick, S. C., McKinney, W. R., Lunt, D. L. T., and Takacs, P. Z., "Using a straightness reference in obtaining more accurate surface profiles," Rev. Sci. Instrum. 63, 1436–1438 (1992); doi: 10.1063/1.1143036..

[13] Irick, S. C., "Improved measurement accuracy in a long trace profiler: compensation for laser pointing instability," Nucl. Instrum. Methods Phys. Res. A 347, 226–230 (1994); https://doi.org/10.1016/0168-9002(94)91882-1.

[14] Takacs, P. Z., Church, E. L., Bresloff, C. J., Assoufid, L., "Improvements in the accuracy and the repeatability of long trace profiler measurements," Appl. Optics 38(25), 5468-5479 (1999).

[15] Senba, Y., Kishimoto, H., Ohashi, H., Yumoto, H., Zeschke, T., Siewert, F., Goto, S., Ishikawa, T., "Upgrade of long trace profiler for characterization of high-precision X-ray mirrors at SPring-8," Nucl. Instrum. and Methods A 616(2-3), 237-240 (2010).

[16] Rommeveaux, A., Hignette, O., Morawe, C., "Mirror metrology and bender characterization at ESRF," Proc. SPIE 5921, 59210N/1-8 (2005).

[17] Rommeveaux, A., Thomasset, M., Cocco, D., "The Long Trace Profilers," in [Modern Developments in X-ray and Neutron Optics], A. Erko, M. Idir, T. Krist, A. G. Michette, Eds., Chapter 10, Springer-Verlag, Berlin/Heidelberg (2008).

[18] Thomasset M., and Polack, F., "Characterization of optical surfaces for the present generations of synchrotron sources," Proc. SPIE 7155, 715506/1-12 (2008).

[19] Kirschman, J. L., Domning, E. E., McKinney, W. R., Morrison, G. Y., Smith, B. V., and Yashchuk, V. V., "Performance of the upgraded LTP-II at the ALS Optical Metrology Laboratory," Proc. SPIE 7077, 70770A/1-12 (2008).
[20] Von Bieren K., "Pencil beam interferometer for aspherical optical surfaces," Proc. SPIE 343, 101-108 (1982).
[21] Takacs, P. Z., Qian, Shinan, "Accuracy limitations in long-trace profilometry," AIP Conf. Proc. 708, 831-834 (2004).
[22] Ali, Z., Artemiev, N. A., Cummings, C. L., Domning, E. E., Kelez, N., McKinney, W. R., Merthe, D. J., Morrison, G. Y., Smith, B. V., and Yashchuk, V. V., "Automated suppression of errors in LTP-II slope measurements with x-ray optics," Proc. SPIE 8141, 81410O-1-15 (2011).
[23] Siewert, F., Buchheim, J., and Zeschke, T., "Characterization and calibration of 2nd generation slope measuring profiler," Nucl. Instrum. Methods A 616(2-3), 119–127 (2010); http://doi.org/10.1016/j.nima.2009.12.033.
[24] Geckeler, R. D. and Just, A. "Optimized use and calibration of autocollimators in deflectometry," Proc. SPIE 6704, 670407-1 – 12 (2007).
[25] Yashchuk, V. V., Artemiev, N. A., Lacey, I., and Merthe, D. J., "Correlation analysis of surface slope metrology measurements of high quality x-ray optics," Proc. SPIE 8848, 88480I-1-15 (2013); doi: 10.1117/12.2024694.
[26] Geckeler, R., Just, A., Krause, M., Yashchuk, V. V., "Autocollimators for Deflectometry: Current Status and Future Progress," Nucl. Instr. and Meth. A 616(2-3), 140-146 (2010).
[27] Geckeler, R. D., Kranz, O., Just, A., and Krause, M., "A novel approach for extending autocollimator calibration from plane to spatial angles," Adv. Opt. Techn. 1(6), 427–439 (2012).
[28] Yashchuk, V. V., "Optimal Measurement Strategies for Effective Suppression of Drift Errors," Rev. Sci. Instrum. 80, 115101-1-10 (2009); http://dx.doi.org/10.1063/1.3249559.
[29] Von Bieren, K., "Pencil Beam Interferometer For Aspherical Optical Surfaces," Proc. SPIE 343, 101 (1982); doi:10.1117/12.933743.
[30] Von Bieren, K., "Interferometry of wave fronts reflected off conical surfaces," Appl. Opt. 22, 2109-2114 (1983); doi: 10.1364/AO.22.002109.
[31] Von Bieren, K., "Pencil beam interferometer," US Patent 4,498,773 (1985).
[32] Takacs, P. Z., Qian, Shi-nan, and Colbert, J., "Design of a Long Trace Surface Profiler," Proc. SPIE 749, 59-64 (1987); doi: 10.1117/12.939842.
[33] Takacs, P. Z., Feng, S. K., Church, E. L., Qian, S., and Liu, W., "Long Trace Profile Measurements On Cylindrical Aspheres," Proc. SPIE 966, 354 (1989); doi:10.1117/12.948082.
[34] Takacs P. Z. and Qian, S. "Surface profiling interferometer," United States Patent No. 4884697 (5 December 1989).
[35] Susini, J., Baker, R., and Vivo, A., "Optical metrology facility at the ESRF," Rev. Sci. Instrum. 66(2),2232-2234 (1995).
[36] Takacs P. Z. and Bresloff, C. J., "Significant Improvements in Long Trace Profiler Measurement Performance," Proc. SPIE 2856, 236-245 (1996); doi:10.1117/12.259878.
[37] Irick, S., "Long trace profiler survey results," Proc. SPIE 3782, 275-282 (1999).
[38] Siewert, F., Assoufid, L., Cocco, D., Hignette, O., Irick, S., Lammert, H., McKinney, W., Ohashi, H., Polack, F., Qian, S., Rah, S., Rommeveaux, A., Schönherr, V., Sostero, G., Takacs, P., Thomasset, M., Yamauchi, K., Yashchuk, V., Zeschke, T., "Global high-accuracy inter-comparison of slope measuring instruments," AIP Conf. Proc. 879, 706-709 (2007) (Daegu, South Korea, May 27 - June 03, 2006).
[39] Yashchuk, V. V., Irick, S. C., MacDowell, A. A., McKinney, W. R., Takacs, P. Z., "Air convection noise of pencil-beam interferometer for long-trace profiler," Proc. SPIE 6317, 63170D-1-12 (2006).
[40] Yashchuk, V. V., Artemiev, N. A., Lacey, I., McKinney, W. R., and Padmore, H. A., "Advanced environmental control as a key component in the development of ultra-high accuracy ex situ metrology for x-ray optics," Opt. Eng. 54(10), 104104/1-14 (2015); doi: 10.1117/1.OE.54.10.104104.
[41] Qian S., and Takas, P., "Wave front-splitting phase shift beam splitter for pencil beam interferometer," Rev. Sci. Instrum. 74(11), 4881-4884 (2003).
[42] Qian S., and Takacs, P., "Equal optical path beam splitters by use of amplitude-splitting and wavefront-splitting methods for pencil beam interferometer," Proc. SPIE 5193, 79-88 (2004).
[43] Centers, G., Smith, B. V., and Yashchuk, V. V., "New operational mode of the pencil beam interferometry based LTP," Proc. SPIE 9962, 996202/1-13 (2016); doi:10.1117/12.2238298.
[44] Senba, Y., Kishimoto, H., Ohashi, H., Yumoto, H., Goto, S. and Ishikawa, T., "Present status of upgraded long trace profiler for characterization of high-precision X-ray mirrors at SPring-8," Proc. SPIE 7801, 780104 (2010).

[45] Yashchuk, V. V., Artemiev, N. A., Centers, G., Chaubard, A., Geckeler, R. D., Lacey, I., Marth, H., McKinney, W. R., Noll, T., Siewert, F., Winter, M., and Zeschke, T., "High precision tilt stage as a key element to universal test mirror for characterization and calibration of slope measuring instruments," Rev. Sci. Instrum. 87(5), 051904 (2016); doi: 10.1063/1.4950729.
[46] Geckeler R. D., and Just, A., "Optimized use and calibration of autocollimators in deflectometry," Proc. SPIE 6704, 670407/1-12 (2007).
[47] Alcock, S. G., Bugnar, A., Nistea, I., Sawhney, K., Scott, S., Hillman, M., Grindrod, J., and Johnson, I., "A novel instrument for generating angular increments of 1 nanoradian," Rev. Sci. Instrum. 86(5), 125108 (2015); http://dx.doi.org/10.1063/1.4937352.
[48] Yashchuk, V. V., McKinney, W. R., Warwick, T., Noll, T., Siewert, F., Zeschke, T., and Geckeler, R. D., "Proposal for a Universal Test Mirror for Characterization of Slope Measuring Instruments", Proc. SPIE 6704, 67040A-1-12 (2007).
[49] Polack, F., Thomasset, M., Brochet, S., and Rommeveaux, A., "An LTP stitching procedure with compensation of instrument errors: Comparison of SOLEIL and ESRF results on strongly curved mirrors," Nucl. Instr. and Met. A 616(2-3), 207-211 (2010).
[50] Nicolas, J., Pedriera, J., Sics, I., Ramirez, C., and Campos, J., "Nanometer accuracy with continuous scans at the ALBA-NOM," Proc. SPIE 9962, Advances in Metrology for X-Ray and EUV Optics VI, 996203 (2016); doi:10.1117/12.2238128.
[51] Yashchuk, V. V., "Positioning errors of pencil-beam interferometers for long trace profilers," Proc. SPIE 6317, 63170A/1-12 (2006).
[52] Irick, S., "Error reduction techniques for measuring long synchrotron mirrors," Proc. SPIE 3447, 101-108 (1988).
[53] Lesso, J. P. and Padgett, M. J., "Dove prisms and polarised light," J. Modern Opt. 46(2), 175–179 (1999). doi:10.1080/09500349908231263.
[54] Moreno, I., "Jones matrix for image-rotation prisms (PDF)," Appl. Opt. 43, 3373-3381 (2004).
[55] Moreno, I., Paez, C., and Strojnik, M., "Polarization transforming properties of Dove prisms," Opt. Commun. 220, 257-268 (2003).
[56] Senba, Y., Kishimoto, H., Miura, T., and Ohashi, H., "Development of a long trace profiler at SPring-8 using a newly developed slope sensor," Proc. SPIE 9962, 996204 (2016); doi: 10.1117/12.2239394.